Abelson Phosphorylation of CLASP2 Modulates its Association With Microtubules and Actin

RESEARCH ARTICLE
Cytoskeleton, March 2014 71:195–209 (doi: 10.1002/cm.21164)
Published 2014 Wiley Periodicals, Inc.†

Abelson Phosphorylation of CLASP2 Modulates its Association With Microtubules and Actin

Ulrike Engel,[1,2†] Yougen Zhan,[1†] Jennifer B. Long,[1] Scott N. Boyle,[3] Bryan A. Ballif,[1] Karel Dorey,[4] Steven P. Gygi,[1] Anthony J. Koleske,[3] and David VanVactor[1*]

[1]Department of Cell Biology, Harvard Medical School, Boston, Massachusetts
[2]Nikon Imaging Center, the University of Heidelberg, Bioquant, 69120 Heidelberg, Germany
[3]Department of Molecular Biophysics and Biochemistry, Yale University, New Haven, Connecticut
[4]Faculty of Life Sciences-Michael Smith Building, University of Manchester, Oxford Road, M13 9PT Manchester, United Kingdom

Received 4 June 2013; Revised 21 December 2013; Accepted 30 December 2013
Monitoring Editor: Bruce Goode

The Abelson (Abl) non-receptor tyrosine kinase regulates the cytoskeleton during multiple stages of neural development, from neurulation, to the articulation of axons and dendrites, to synapse formation and maintenance. We previously showed that Abl is genetically linked to the microtubule (MT) plus end tracking protein (+TIP) CLASP in *Drosophila*. Here we show in vertebrate cells that Abl binds to CLASP and phosphorylates it in response to serum or PDGF stimulation. In vitro, Abl phosphorylates CLASP with a Km of 1.89 μM, indicating that CLASP is a *bona fide* substrate. Abl-phosphorylated tyrosine residues that we detect in CLASP by mass spectrometry lie within previously mapped F-actin and MT plus end interaction domains. Using purified proteins, we find that Abl phosphorylation modulates direct binding between purified CLASP2 with both MTs and actin. Consistent with these observations, Abl-induced phosphorylation of CLASP2 modulates its localization as well as the distribution of F-actin structures in spinal cord growth cones. Our data suggest that the functional relationship between Abl and CLASP2 is conserved and provides a means to control the CLASP2 association with the cytoskeleton.

Additional Supporting Information may be found in the online version of this article.

†The first two authors contributed equally to this work.

Bryan A. Ballif's present address is Department of Biology, University of Vermont, Burlington, VT 05405

*Address correspondence to: David VanVactor, Department of Cell Biology, Harvard Medical School, Boston, MA 02115, USA.
E-mail: davie_vanvactor@hms.harvard.edu

Published online 12 March 2014 in Wiley Online Library (wileyonlinelibrary.com).

Key Words: Abelson kinase; Abl; CLASP; tyrosine phosphorylation; microtubule

Introduction

Coordinated control of cytoskeletal dynamics is critical for cell morphogenesis, cell division, and cell migration [Rodriguez et al., 2003; Kodama et al., 2004; Heng and Koh, 2010]. Inside the cell, two cytoskeletal polymers with distinct properties mediate key aspects of cell movement: peripheral microfilament networks that drive local membrane protrusion and central microtubule (MT) arrays that organize organellar traffic and long-range cell structure. Although ample evidence has demonstrated coupling between MT and F-actin networks, the mechanisms that achieve such coordination are still emerging. One class of MT regulators, the MT plus end tracking proteins (MT+TIPs), are spatially and biochemically poised at the interface between growing MTs and peripheral F-actin structures at or near the membrane cortex where responses to extracellular signals are transduced [Gundersen, 2002; Jiang and Akhmanova, 2011]. CLASP (Cytoplasmic Linker Protein [CLIP] Associated Protein) is a highly conserved member of the MT+TIP proteins that localizes at or near the MT plus end [Akhmanova et al., 2001]. Through direct interactions with tubulin, CLASP is thought to stabilize MTs by reducing catastrophe frequency in the cell periphery during directional cell migration [Mimori-Kiyosue et al., 2005; Drabek et al., 2006; Efimov et al., 2007]. CLASP is also involved in the generation of trans-Golgi-derived MTs [Efimov et al., 2007; Miller et al., 2009].

Several vertebrate CLASP proteins have been identified including CLASP1, and two isoforms CLASP2α and CLASP2γ from a second gene expressed predominantly in the nervous system [Akhmanova et al., 2001]. Previous studies have demonstrated that a central sequence in

CLASP2α from amino acids 677–813 is required for MT plus end binding whereas a neighboring domain from amino acids 1031–1240 is essential for MT lattice binding [Mimori-Kiyosue et al., 2005; Wittmann and Waterman-Storer, 2005]. CLASP2 can also bind directly to actin filaments [Tsvetkov et al., 2007], although the regulation of the CLASP–actin interaction is not understood. Interestingly, CLASP knock down in *Xenopus* spinal cord axons results in abnormalities in F-actin structure [Marx et al., 2013]. Moreover, several actin-associated factors and actin-MT crosslinking proteins are part of the genetic interactome of the *Drosophila* CLASP homolog (known as Chromosome bows [Chb]/Orbit/Multiple Asters [MAST]) [Lowery et al., 2010], suggesting that CLASP may directly or indirectly link actin and MTs in the cell periphery.

CLASP and other MT+TIPs are likely to respond to multiple cellular signals. For example, CLASP binding to MT lattice sites near MT plus ends at the cell's leading edge is regulated by serum exposure [Akhmanova et al., 2001]. It has been shown that the affinity of CLASP2α binding to MTs can be regulated by GSK3β-induced phosphorylation on several serine/threonine phospho-acceptor residues [Akhmanova et al., 2001; Wittmann and Waterman-Storer, 2005; Kumar et al., 2009]. However, additional regulatory mechanisms for controlling CLASP function in different contexts are likely to exist. Using in vivo genetic screens for components that modulate the function of the Abelson (Abl) kinase pathway, *Drosophila* CLASP was identified as a key factor required for accurate guidance of embryonic axons [Lee et al., 2004]. The Abl family, including c-Abl and the Abl-related gene (Arg) in vertebrates and a single ortholog in *Drosophila*, are non-receptor tyrosine kinases that serve many cellular functions, including neurogenesis, cell migration, and neuronal morphogenesis [Moresco et al., 2003; Hernandez et al., 2004]. Abl's role in controlling embryonic axonal development was first discovered in *Drosophila* [Gertler et al., 1989; Elkins et al., 1990; Wills et al., 1999a,b] and has been linked to many different axon guidance receptor families in this model organism, including Fasciclin I, Roundabout (Robo), and Leukocyte-Antigen Related (LAR) families [Wills et al., 1999a; Bashaw et al., 2000]. Studies in vertebrates highlight the breadth of signaling pathways that require Abl, including axon guidance receptors (e.g., Ephrin/Eph, Semaphorin) [Yu et al., 2001; Toyofuku et al., 2004; Harbott and Nobes, 2005; Shimizu et al., 2008], receptors for growth factors (e.g., epidermal growth factor [EGF], platelet-derived growth factor [PDGF]) [Plattner et al., 1999], and receptors for extracellular matrix components (e.g., Integrins, LAR) [Wills et al., 1999a; Moresco et al., 2005]. Downstream of receptor activation, Abl activity is enhanced by auto-phosphorylation or via phosphorylation by Src family kinases [Tanis et al., 2003] during actin-based cell ruffling in response to cues such as PDGF or EGF [Plattner et al., 1999]. Within the cell, Abl binds to and phosphorylates substrates with diverse cellular functions. For example, in *Drosophila*, Abl regulates the action of Enabled (Ena), influencing actin dynamics [Gertler et al., 1995; Wills et al., 1999a; Bear et al., 2000; Baum and Perrimon, 2001]. While Abl family kinases are highly conserved across species [Colicelli, 2010], the degree to which functional relationships between Abl and its effector proteins are conserved from vertebrate to invertebrate has not been extensively tested.

In our previous genetic studies, we showed that *Drosophila* CLASP is required for Abl function in motor axons [Lee et al., 2004]. Although this in vivo analysis was the first to link CLASP and Abl function in any context, genetic analysis alone cannot reveal whether the interaction between CLASP and Abl is direct or indirect. In addition, our genetic epistasis experiments did not conclusively show that CLASP is regulated downstream of the kinase. Moreover, although CLASP and Abl sequences are highly conserved across species, the question remained as to whether the functional relationship between CLASP and Abl is retained in vertebrate cells. Using biochemical assays with vertebrate cells and proteins, we now address these questions using the neuronal-enriched gene CLASP2. We find that Abl binds to and phosphorylates CLASP2 in response to extracellular signals such as serum or PDGF. In vitro experiments indicate that CLASP2 is a direct substrate of Abl. Biochemical experiments with purified proteins show that Abl can modulate CLASP2 binding to MTs and actin. Finally, analysis of CLASP2 in cultured vertebrate neurons reveals that Abl regulates CLASP2 localization and its interaction with both MTs and actin in the growth cone. Together our findings suggest that a functional relationship between Abl and CLASP2 is conserved across species that this may coordinate actin and MT behavior.

Results

Signal-Dependent Abl Phosphorylation and Association of CLASP2

Our previous genetic analysis showed that Abl requires CLASP function for efficient axon guidance signaling in *Drosophila* motor axons [Lee et al., 2004]. While many different mechanisms could account for this functional relationship in the cell, perhaps the most obvious possibility was that CLASP acts as a downstream target of Abl signaling activity. To investigate whether vertebrate CLASP2 is responsive to Abl kinase activity, we first performed cell-based phosphorylation assays. A green fluorescent protein (GFP)-CLASP2α fusion was transfected into HEK 293T cells in the presence or absence of Abl-PP (Fig. 1), a constitutively active Abl kinase mutant [Barila and Superti-Furga, 1998]. Immunoprecipitation (IP) of GFP-CLASP2α expressed in HEK 293T cells using anti-GFP antibodies was performed to improve sensitivity. Many different

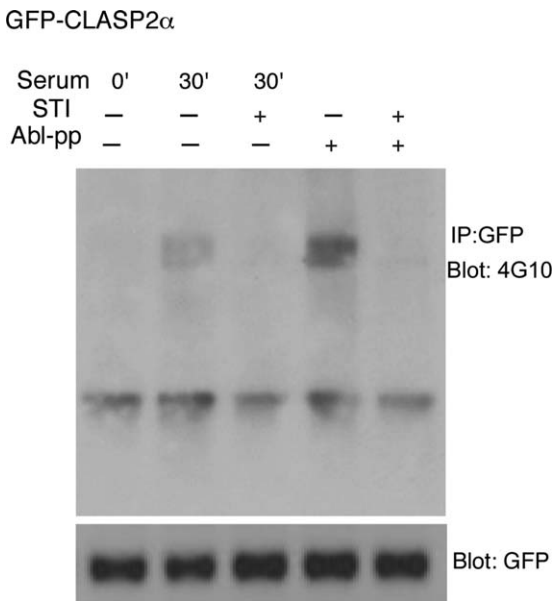

Fig. 1. CLASP2 is tyrosine-phosphorylated by Abl kinase. GFP-CLASP2α was immunoprecipitated from transfected HEK293T cells following starvation and serum treatment for 30 min in the presence or absence of STI-571 (1 μM), a specific Abl inhibitor. Abl-PP is a constitutively active Abl kinase and was co-transfected with GFP-CLASP2α as indicated. Tyrosine phosphorylation of CLASP2α was identified by anti-phosphotyrosine antibody 4G10. The lower band visible in the 4G10 blot is the IgG heavy chain. Re-blotting for GFP shows an equal amount of GFP-CLASP2α immunoprecipitated in each lane.

signals are known to induce Abl kinase activity in different contexts. However, we began with a simple serum starvation and re-exposure assay known to influence CLASP2 behavior [Akhmanova et al., 2001]. Following serum starvation and subsequent serum exposure for 30 min in the absence of Abl-PP (see Materials and Methods), tyrosine phosphorylation of GFP-CLASP2α was observed with the anti-phosphotyrosine (α-pY) antibody 4G10 on Western blots of IPs (the second lane, Fig. 1). This phosphorylation was abolished with treatment with 1 μM of STI-571 (the third lane, Fig. 1). STI-571 is a tyrosine kinase inhibitor with a high selectivity for Abl at 1 μM compared to other cytosolic tyrosine kinases [Druker et al., 1996]. In parallel, when Abl-PP was co-transfected with GFP-CLASP2α, a stronger phosphorylation signal was obtained (the fourth lane, Fig. 1), which was also abolished by treating with 1 μM of STI-571 (Fig. 1). These data suggest that CLASP2α is responsive by tyrosine phosphorylation to at least one factor in serum, and that this is Abl-dependent.

Our observation that Abl activation can lead to CLASP2 phosphorylation raised the possibility that these two proteins might form protein–protein interactions stable enough to be detected by IP. To test this, we used anti-GFP antibodies to IP a GFP-CLASP2α fusion protein expressed in HEK 293T cells. We found that GFP-CLASP2α IP consistently recovers endogenous Abl protein as detected by Western blot (Fig. 2A). To determine whether Abl and CLASP2 can interact directly, we also performed binding of Abl to purified CLASP2 in a gel overlay assay and found that Abl can associate with the relevant CLASP2 bands (data not shown). These data suggest that Abl can associate with CLASP2α, under conditions where CLASP2 expression is not limiting. This prompted us to use IP assays to examine the effects of signaling on CLASP2 association in later experiments.

In order to define a specific serum factor capable of inducing CLASP2 phosphorylation, we tested the PDGF signaling pathway because previous reports showed increased Abl activity in response to PDGF receptor signaling activation and PDGF is abundant in serum [Plattner et al., 1999; Boyle et al., 2007]. Starved cells were treated with serum and protein extracts were assayed at different time points. Abl protein recovered from HEK293T cells by IP using anti-Abl antibodies showed increased phosphorylation at 2 and 5 min after serum addition when probed with 4G10 (see Supporting Information Fig. S1), whereas the addition of a PDGF receptor-selective inhibitor (Tyrphostin, AG 1296) at a final concentration of 1 μM reduced the phosphorylation of Abl at these time intervals (see Supporting Information Fig. S1). These data suggested that PDGF signaling induces phosphorylation of Abl in this system. Since tyrosine phosphorylation of Abl can greatly enhance its kinase activity [Tanis et al., 2003], our findings raised the possibility that phosphorylation of CLASP2α in response to serum is partially mediated through PDGF receptor signaling.

Having examined PDGF stimulation of Abl phosphorylation in our cell-based system, we next asked whether direct PDGF exposure to cells could lead to CLASP2 phosphorylation. Recombinant PDGF-BB was applied at 100 ng/ml to the cultured cells followed by Abl IP and Western blot analysis. Treatment with PDGF for 5 min induced increased Abl phosphorylation as indicated by the 4G10 antibody, whereas Abl protein level did not change (Fig. 2B). Moreover, PDGF treatment also enhanced the association of CLASP2α with Abl, because an increased amount of CLASP2α co-immunoprecipitated with Abl (Fig. 2C) as detected by antisera to CLASP2α (a gift from Dr. Anna Akhmanova). Increased CLASP2α tyrosine phosphorylation was also observed by probing Western blots with 4G10 (Fig. 2C). Therefore, our data suggest that PDGF signaling leads to activation of Abl, increased phosphorylation of CLASP2, and enhanced CLASP2 binding to Abl.

CLASP is a Direct Substrate of the Abl Kinase

CLASP2γ and CLASP2α are highly conserved isoforms that share all of the known CLASP2 protein interaction domains, differing only at the N-terminus where CLASP2α contains a 233 amino acid insertion. To test whether the sequences in common between these CLASP2 isoforms can be phosphorylated in an Abl kinase-dependent fashion, a CLASP2γ -myc construct was transfected into COS7 cells in the presence or absence of constitutively active Abl-PP (Fig. 3A).

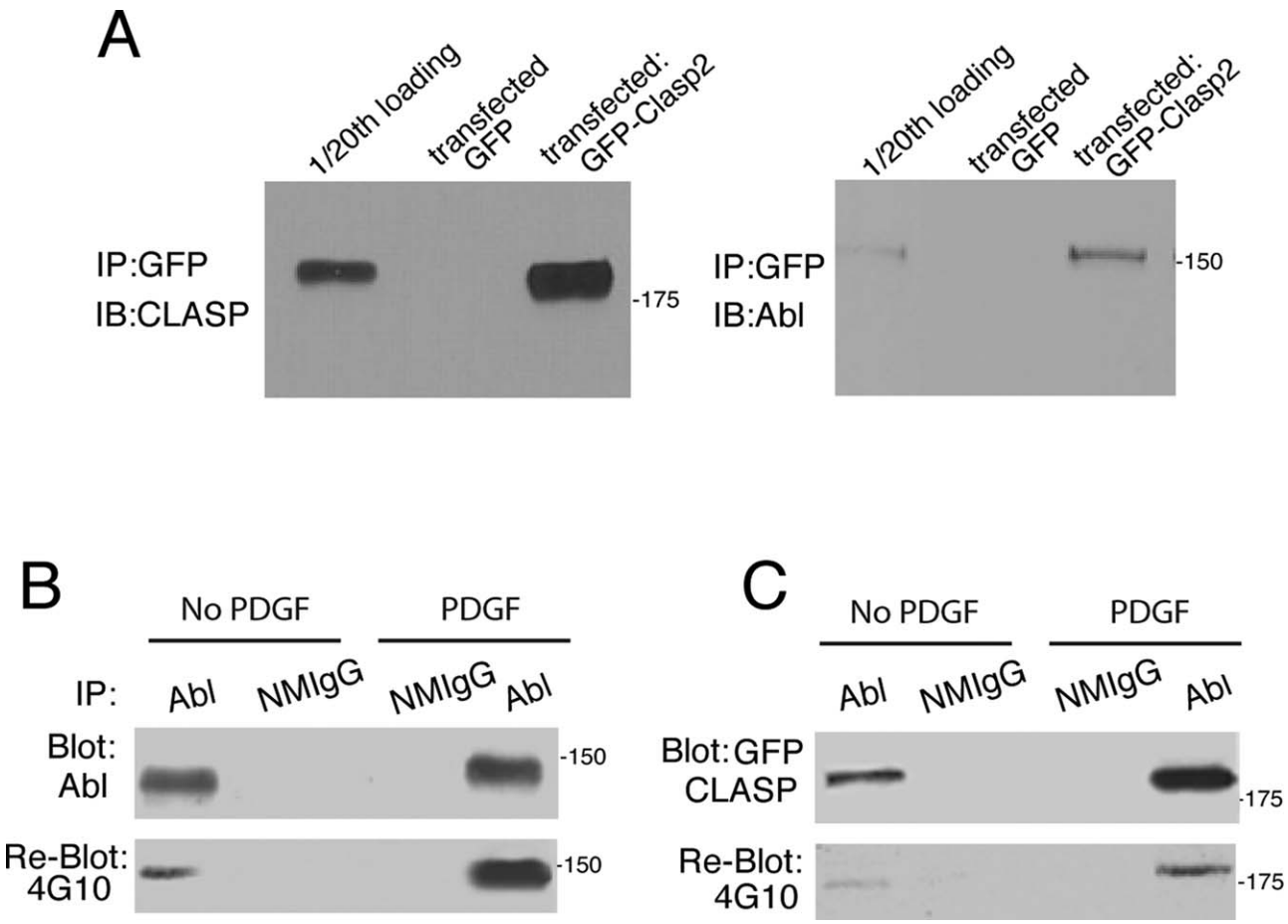

Fig. 2. CLASP2 phosphorylation and interaction with Abl are enhanced by PDGF treatment. A: CLASP2α is associated with endogenous Abl. Lysates from HEK293T cells transfected with either GFP-CLASP2α or GFP (as indicated above lanes) were immunoprecipitated with anti-GFP antibody, probed with anti-CLASP2 (a gift from Anna Akhmanova left panel), stripped and reprobed with anti-Abl antibody (right panel). 1/20th of lysates from cells transfected with GFP-CLASP2α were loaded as controls. **B:** Increased phosphorylation of Abl after PDGF stimulation. Abl was immunoprecipitated from GFP-CLASP2α transfected 293T cells, which were serum starved and subsequently treated with PDGF for 5 min. A similar level of Abl was immunoprecipitated with and without stimulation (upper panel anti-Abl) while its phosphorylation was increased significantly after PDGF treatment as revealed by anti-phosphotyrosine antibody 4G10 (lower panel). **C**: PDGF increases association between Abl and CLASP2. Upper panel shows CLASP2 immunoprecipitated by Abl antibody. Lower panel shows phosphorylated CLASP2 by 4G10. GFP transfection alone does not change 4G10 signal (data not shown).

CLASP2γ-myc showed an electrophoretic mobility shift to higher apparent molecular weight when co-expressed with Abl-PP (Fig. 3A). Addition of the Abl inhibitor STI-571 prevented this shift, indicating kinase-dependence. To verify that the change in apparent molecular weight was due to phosphorylation, we added calf intestinal phosphatase (CIP) to extracts containing CLASP2γ-myc expressed with Abl-PP. CIP eliminated the slower migrating isoforms, shifting CLASP2 to a lower apparent molecular weight (Fig. 3A). This difference in apparent molecular weight suggests that CLASP2γ-myc is phosphorylated in an Abl-dependent fashion; the magnitude of the shift also suggests multiple sites of baseline phosphorylation by other kinases such as GSK-3β in these cultured cells [Wittmann and Waterman-Storer, 2005; Kumar et al., 2009].

Our cell-based data indicated that CLASP2 phosphorylation was responsive to Abl, but we performed in vitro kinase assays to test whether Abl phosphorylated purified recombinant CLASP2γ directly. We found that Abl phosphorylated CLASP2γ with rapid kinetics reaching maximal phosphorylation in less than 20 min (Fig. 3B). We utilized steady-state kinetic analysis to compare Abl-CLASP2 phosphorylation with other known Abl substrates. Interestingly, when we varied the concentration of CLASP2γ in the presence of a fixed concentration of Abl kinase (10 nM kinase) and measured incorporation of radiolabeled phosphate we found evidence of cooperativity in the CLASP2 phosphorylation. Fitting these data to the Hill equation (Fig. 3C), we calculated a Hill coefficient of 4.2 ± 0.2 (Abl; Fig. 3D), k_{cat} of 65.9 ± 9.4 min^{-1} and K_m of 0.717 ± 0.008 μM. The k_{cat} for CLASP phosphorylation by Arg under the same conditions was comparable (44.2 ± 7.3 min^{-1}; data not shown) consistent with previous observations that Abl and Arg have similar abilities to phosphorylate distinct

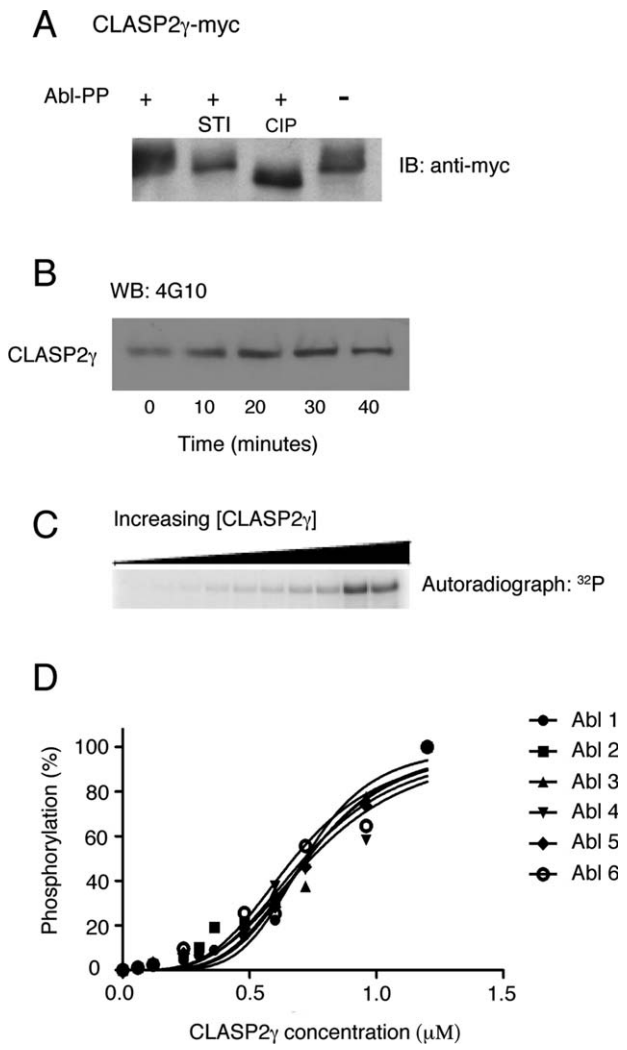

Fig. 3. Phosphorylation of CLASP2γ by Abl in cells and in vitro. A: CLASP2γ is phosphorylated by Abl-PP in Cos-7 cells. Co-expression of the constitutive active Abl-PP reduces the mobility of CLASP2γ-myc in SDS-electrophoresis. This mobility is slightly enhanced by treatment of cells with STI-571. Treatment of cell lysates with CIP enhances the mobility in SDS-gels even further, suggesting CIP further de-phosphorylate CLASP2γ. **B:** In vitro phosphorylation of CLASP (25 nM) by purified Abl (10 nM) was assayed by 4G10 signal. Both recombinant proteins were produced and purified using a baculoviral expression system. **C:** Increasing concentrations of purified His-CLASP2γ were incubated with 10 nM recombinant Abl in the presence of γ-p^{32}ATP. **D:** Quantification of concentration dependence by normalized pixel intensity shows a sigmoidal relationship between substrate concentration and phosphorylation. Data from six independent experiments are shown. Data were fit to the Hill equation ($V_o = V_{max} \times [S]^h / (K_m^h + [S]^h)$) with $R^2 = 0.96$.

substrates in vitro [Tanis et al., 2003]. These values are within the range of other previously characterized Abl/Arg substrates [Tanis et al., 2003; Boyle et al., 2007]. The cooperativity may represent some phosphorylation-dependent aspect of the CLASP2–Abl interaction, since CLASP has been reported to be monomeric in other studies [Patel et al., 2012].

Identification of CLASP Residues Phosphorylated by Abl Kinase

A number of functional domains have been defined in mammalian CLASP2 proteins [Komarova et al., 2002; Wittmann and Waterman-Storer, 2005; Tsvetkov et al., 2007; Patel et al., 2012]. In order to generate testable hypotheses regarding the possible impact of Abl phosphorylation on CLASP2 function, we set out to map phosphoacceptor sites that might be common to both CLASP2 isoforms. We first compared the activity of Abl-PP on several GFP-CLASP2γ deletion constructs in COS7 using the α-pY antibody 4G10 (Figs. 4A and 4B). We found that most phosphorylation signals are located within a 537 amino acid [aa] domain (CLASP2α aa 712–1248; Fig. 4A). This region of CLASP2 contains domains responsible for direct MT-binding: the domain required for MT+TIP localization (aa 677–813) and a more C-terminal a domain binding MT lattice (aa 1031–1240) [Mimori-Kiyosue et al., 2005; Wittmann and Waterman-Storer 2005]. Interestingly, the central MT+TIP binding domain was also one of the domains showing actin interaction in fibroblast lysates [Tsvetkov et al., 2007].

Having roughly mapped Abl-dependent phosphorylation sites in the region of aa 712–1248 by gel shift (not shown) and by Western blot (Fig. 4B), we then proceeded to use tandem ion-trap mass spectrometry (MS/MS) to identify specific phosphoacceptor residues in the CLASP2 sequence. Multiple rounds of phosphorylation mapping were performed: (i) MS/MS analysis of CLASP2γ phosphorylated in vitro with recombinant c-Abl, (ii) MS/MS analysis of CLASP2γ immunoprecipitated from Abl-PP expressing HEK293T and Cos7 cells, and (iii) MS/MS analysis of GFP-CLASP2α immunoprecipitated from HEK293T cells exposed to serum after a period of serum-starvation. Within the central MT+TIP binding domain (aa 677–813) common to both CLASP2 isoforms, two Abl phosphorylation site residues were identified in these experiments: Y800 and Y807 that are both conserved among mammalian species (CLASP2α numbering; Figs. 4A and 4C, Supporting Information Fig. S2). The location of these residues within the MT+TIP domain raised the intriguing possibility that Abl might regulate CLASP-MT interaction and localization.

Abl Phosphorylation Modifies CLASP Association With MTs

Although CLASP2 function can be assessed with a variety of approaches, it was important for us to utilize methodology that could measure an activity of CLASP that might be modulated by Abl directly. For this reason, we selected an in vitro assay where the MT-binding activity of CLASP2 could be monitored using purified components in the same buffer conditions used in our kinase assays. MTs were first polymerized and then stabilized with taxol, followed by incubation with purified proteins (myc-tagged CLASP2α

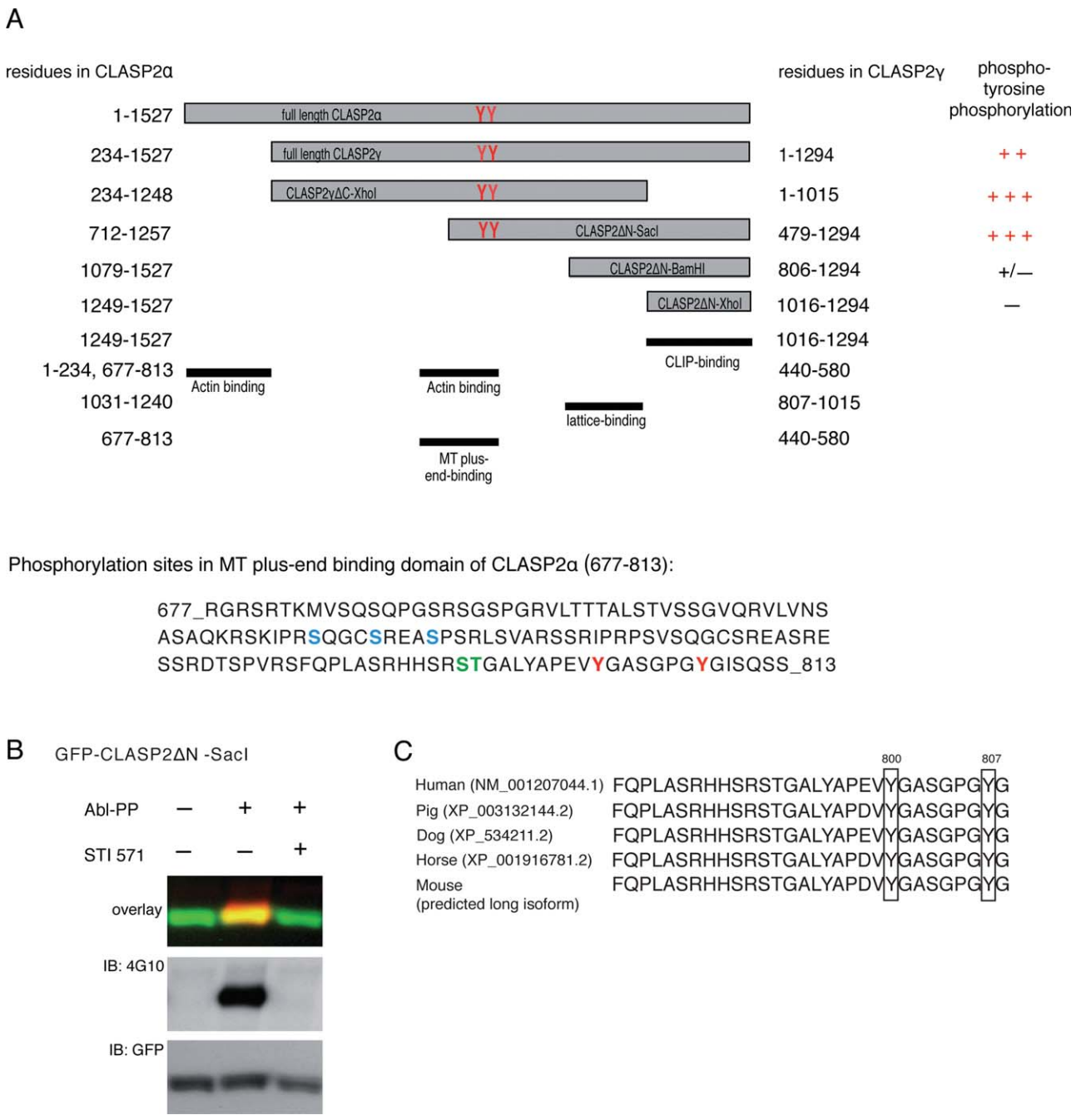

Fig. 4. Identification of CLASP2 tyrosine phosphorylation sites. A: Schematic representation of human CLASP2 constructs and levels of tyrosine phosphorylation. Several N-terminal and C-terminal truncations of CLASP2γ fused to EGFP were tested for in vitro phosphorylation in Cos-7 cells (see B) and the region between the SacI and BamHI restriction sites was identified to be necessary for efficient phosphorylation. This contains the domain necessary for plus end binding (CLASP2-M, [Mimori-Kiyosue et al., 2005]) which was also shown to bind actin [Tsvetkov et al., 2007]. Within this domain the phospho-tyrosines identified by mass spec analysis of full length CLASPα, after serum induction Y800 and Y807, are highlighted in red. Significant phosphorylation of serine 790 or threonine 791 (shown in green) was also observed. The tyrosines identified in mass spec are downstream of two cassettes of GSK-phosphorylation sites (here shown in blue [Kumar et al., 2009]). **B:** GFP-CLASP fusions were expressed in Cos-7 cells together with Abl-PP and analyzed after IP for tyrosine phosphorylation levels by 4G10 antibody. The results for several truncations of CLASP2 are summarized in A. **C:** The region containing phosphotyrosines Y800 and Y807 is conserved across many mammalian CLASP2 isoforms and the individual sequences are shown here. Also shown is the predicted region for mouse CLASP2β. Total RNA was harvested from a variety of embryonic mouse tissues, reverse transcribed, and PCR performed for CLASP2. In all neuronal tissues tested (brain, spinal cord, dorsal root ganglion), sequencing of the amplified region identified both a short and long isoform that differed in this phosphotyrosine containing region (data not shown).

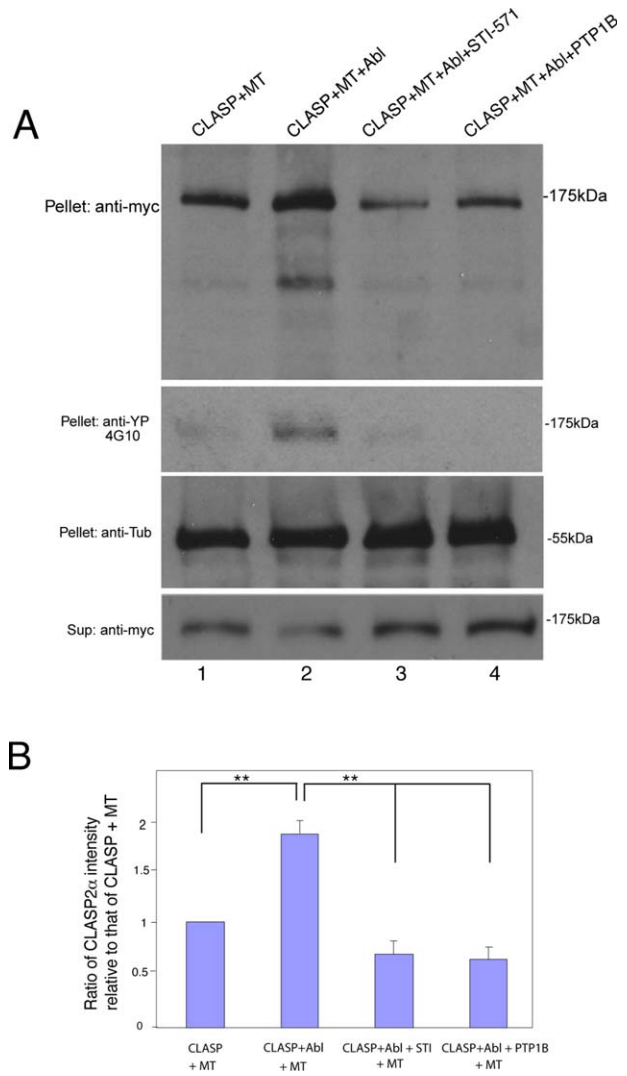

Fig. 5. Modulation of CLASP2α binding to MTs by Abl kinase. Purified CLASP2α-myc-His was incubated with taxol-stabilized MT bundles (see Materials and Methods) for 30 min with the components indicated above the lanes. The mixture was centrifuged and the pellet was collected and analyzed by Western blot using an antibody directed against myc to detect CLASP2α. Blots were re-probed with the anti-phosphotyrosine antibody 4G10 and anti-tubulin (anti-tub). Increased amounts of CLASP2α were pelleted with stabilized MTs in the presence of Abl (Lane 2) compared to the absence of Abl (Lane 1), STI-571 treatment (Lane 3), or protein tyrosine phosphatase 1B (PTP1B) (1 μg/μl) treatment (Lane 4). In Lanes 3 and 4 more stabilized MTs were present in the reaction than in Lanes 1 and 2. Additional stabilized MTs were added to the reaction and pelleted in Lanes 3 and 4. Sup: supernatants. **B:** Quantification of blots shown in (A). Error bars represent standard error of the mean, $^{**}P < 0.01$. [Color figure can be viewed in the online issue, which is available at wileyonlinelibrary.com.]

purified from HEK 29T3 cells), before being centrifuged at 100,000 × *g* to pellet MT polymers (see Materials and Methods). Subsequent Western blot analysis of separate soluble (supernatant) and insoluble (pellet) fractions and comparison of protein content at the relevant molecular weights allowed us to assess myc-tagged CLASP2α binding to MT polymers in the presence or absence of Abl kinase activity. CLASP2α alone was enriched with tubulin in the pellet fraction (Lane 1, Fig. 5A). CLASP2α without MTs in the same buffer conditions remained in the supernatant (Supporting Information Fig. S3). Because MTs do not display dynamic instability in the presence of taxol, the association of CLASP2α with MTs in this assay is likely to reflect only MT lattice interaction.

We then examined the effect of adding Abl kinase. Interestingly, the association of CLASP2α with MTs was significantly increased in the pellet and decreased in the supernatant when Abl was added (Lane 2, Fig. 5A) compared with CLASP2α in the absence of Abl (Lane 1, Fig. 5A; quantified in Fig. 5B). In order to confirm that Abl kinase activity is essential to the enhanced MT binding of CLASP2α, we compared the effect of Abl added in the presence of the inhibitor STI-571 (Lane 3, Fig. 5A). We also performed a parallel experiment using dual specificity protein phosphatase PTP1B to eliminate protein phosphorylation in the purified input proteins (Lane 4, Fig. 5). Both STI-571 and PTP1B decreased CLASP2α association with MTs dramatically in the presence of Abl kinase (quantified in Fig. 5B), suggesting that phosphorylation is required for the change in binding. Because these treatments reduce CLASP2-MT binding to levels slightly below the initial input protein, we believe that the input CLASP2α was partially phosphorylated by endogenous kinases in the host cells before purification. Consistent with this notion, comparison of CLASP2α under each condition using the 4G10 antibody revealed a high level of tyrosine phosphorylation when Abl alone was present, but also detected a low signal for the input protein and in the STI-571-treated control (compare Lanes 2 to 1 and 3, Fig. 5A).

Abl Regulates CLASP2α Interaction With Actin

Because Abl-family kinases control both MT and actin effector proteins and can localize at the interface between the two polymer arrays in motile cells [Miller et al., 2004], and because CLASP2 itself can bind to both MTs and F-actin [Tsvetkov et al., 2007], we wondered if Abl phosphorylation of CLASP2 might also regulate interactions between CLASP2 and actin. Using an F-actin pelleting assay similar to the MT binding assay (see Materials and Methods), we asked whether CLASP2 associated with F-actin in vitro. We found that purified CLASP2 displayed a low but reproducible association with pelleted F-actin (Lane 2, Fig. 6A). However, when recombinant Abl was added to the assay, we found a marked increase in the binding of CLASP2 to the actin pellet (Lane 3, Fig. 6A). Because this increase in association was eliminated by co-incubation with the inhibitor STI-571 (Lane 4, Fig. 6A) or phosphatase (Lane 5, Fig. 6A), we concluded that kinase activity was required for the change in binding.

Our in vitro assays suggesting parallel effects of Abl on CLASP raised the question of whether CLASP might

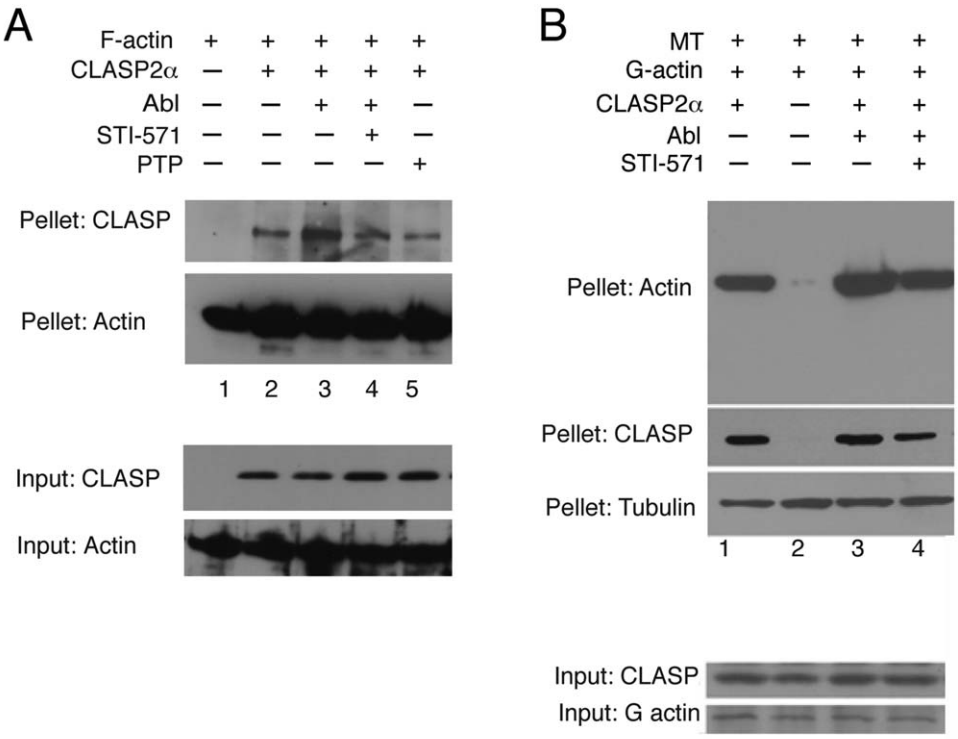

Fig. 6. Abl regulates CLASP2 binding to microfilaments. A: F-actin filaments were incubated with purified CLASP-myc-His with or without Abl and other reagents as indicated above lanes. After centrifugation, equal amounts of pellet (top panel) and the input (lower panel) were analyzed for each treatment with antibodies to actin, anti-myc for detection of CLASP2α-myc-His, and anti-tubulin. **B**: Purified CLASP2α-myc-His was incubated with taxol-stabilized MT bundles (see Materials and Methods) for 30 min with the components indicated above lanes. Monomeric (G) actin was added to the reaction instead of filamentous (F) actin. The mixture was centrifuged and the pellet was collected and analyzed by Western blot using antibodies directed against actin, tubulin, and myc (to detect CLASP2α). G-actin pellets with MTs in the presence of CLASP2α (Lane 1), but not in the absence of CLASP2 (Lane 2). Abl enhances the association of G-actin with MTs (Lane 3) and this association is abolished with STI-571 (Lane 4). Bottom panels show the input (1/10 of the total reaction volume) of both CLASP and G-actin.

simultaneously interact with actin and MTs. Because F-actin and MTs would pellet together even without CLASP, we asked whether CLASP2 might shift the distribution of monomeric (G)-actin in the MT pelleting assay. We incubated taxol-stabilized MTs with purified CLASP2α or in the presence of G-actin and found that G-actin and MTs associated in the presence (Lane 1, Fig. 6B) but not in the absence of CLASP2α (Lane 2, Fig. 6B). Moreover, addition of active Abl kinase increased this association (Lane 3, Fig. 6B), but not in the presence of STI-571 (Lane 4, Fig. 6B). Together, our assays with purified proteins suggested that Abl can alter CLASP2 interactions with MTs and actin, raising the question of what effects Abl might have in an intact cell.

Activated Abl Induces a Shift in CLASP2 Subcellular Localization

Our previous imaging of CLASP2 expression and localization in *Xenopus* spinal cord neurons demonstrated that CLASP2 decorates a subset of "pioneer" MT plus ends which track along bundles of actin [Lee et al., 2004]. To test the effect of Abl kinase activity on CLASP2 behavior in the cell, we co-expressed GFP-CLASP2 with hyperactive Abl-PP in *Xenopus* growth cones. At this high level of Abl activity we discovered striking changes in CLASP2 localization (Figs. 7A, 7B, and 7D, Supporting Information Movie S1). First, examination of MT plus ends showed that Abl-PP expression reduced the number of detectable CLASP2 comets by approximately threefold compared to controls (compare Figs. 7A–7E and Supporting Information Movies S1–S2; quantified in Fig. 7C). This Abl-induced change in CLASP2 MT+TIP comets was abolished by STI571, indicating that it was strictly phosphorylation-dependent (Fig. 7F, Supporting Information Movie S3). The change in CLASP2 plus end tracking was not due to a lower MT density, as tubulin staining showed dense arrays of MTs in these growth cones (data not shown). Due to the reduction of CLASP2 plus end localization, we measured MT dynamics by manual tracking of CLIP-170 localization in Abl-PP-expressing growth cones. Interestingly, the rate of plus end translocation marked by CLIP-170 was not significantly different from control growth cones (Supporting Information Figs. S4C, S4D, and S4E). However, we did observe a

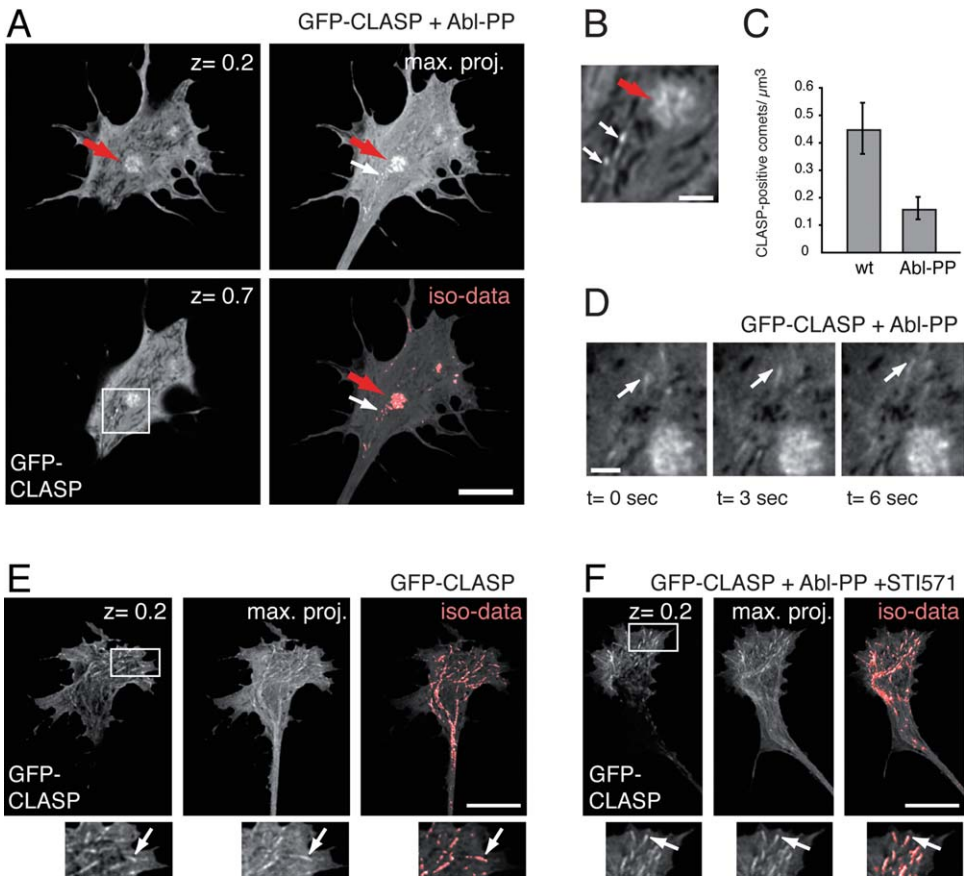

Fig. 7. High Abl-activity relocalizes CLASP to Abl induced growth cone adhesive plaques. CLASP2 localization in neuronal growth cones depends on Abl activity. Live growth cones expressing indicated constructs were subjected to fast optical sectioning by spinning disk confocal microscopy followed by deconvolution for better localization accuracy. The resulting image stacks are displayed as single optical slices (z distance to substrate in µm is indicated) and as maximum projection through the stack (max. proj.); the result of a 3D thresholding is overlaid in red (iso-data). **A:** GFP-CLASP2γ (GFP-CLASP) co-expression with constitutive active Abl (Abl-PP) results in accumulation of GFP-CLASP2γ in the middle of the growth cone (red arrows) close to the substrate ($z = 0.2$ and $z = 0.7$), only weak residual MT plus end tracking is detected (white arrows, see also Supporting Information Movie S2). **B:** Enlarged insert of A (plane $z = 0.7$) indicates GFP-CLASP2γ accumulation in adhesive plaques (red arrow) and localization to plus ends (white arrows). **C:** Quantification of GFP-CLASP2γ-positive comets per volume in wild type (wt) versus Abl-PP expressing neurons. Error bars represent standard error of the mean. ($P < 0.05$). **D:** Dynamic localization of GFP-CLASP2γ in the same growth cone as shown in A. Arrow follows CLASP2γ-positive growing MT end (see also Supporting Information Movie S1). **E:** GFP-CLASP2γ expressing wild-type growth cone shows typical MT plus end tracking in the periphery (white arrows in insert, see also Supporting Information Movie S2). **F:** GFP-CLASP2γ localization of Abl-PP expressing growth cones treated with 10 µM STI571 is indistinguishable from the localization of GFP-CLASP2γ in the control growth cone in E. Inserts show plus end tracking (see also Supporting Information Movie S3). Scale bars in A, E, and F: 10 µm; in B and D: 2 µm. Magnified inserts in E and F are 10 µm × 5 µm and 9 µm × 5 µm in size, respectively.

striking change in the trajectories of MTs with hyperactive Abl; unlike controls where MTs display frequent co-linearity, MTs lost co-linearity in Abl-PP expressing growth cones (see Supporting Information Figs. S4A–S4D).

Although the reduction in CLASP2 +TIP localization was striking and consistent with the location of phosphoacceptor sites in the +TIP domain, perhaps more conspicuous was a massive re-localization of CLASP2 to large plaques in the central domain of the Abl-PP-expressing growth cones (Fig. 7A; red arrow, see also Supporting Information Movie S1). Interestingly, the plaques also showed accumulation of Abl (Supporting Information Fig. S5C) and appeared to be fixed with respect to the substrate over time (Supporting Information Fig. S5A), suggesting that they were associated with adhesion. Because growth cones appeared somewhat thicker and larger when Abl-PP was expressed, it was important to rule out any possible volume effects when assessing CLASP2 localization. To avoid the potentially misleading summation of fluorescence intensity produced by standard wide field microscopy, we performed optical sectioning on live growth cones with a spinning disk confocal microscope followed by deconvolution for all images shown in Fig. 7 (see Materials and Methods). Using this procedure, GFP-CLASP, but not GFP alone, was localized to the Abl-induced plaques (compare Supporting Information Figs. S5D and S5E). Moreover, cross-sections

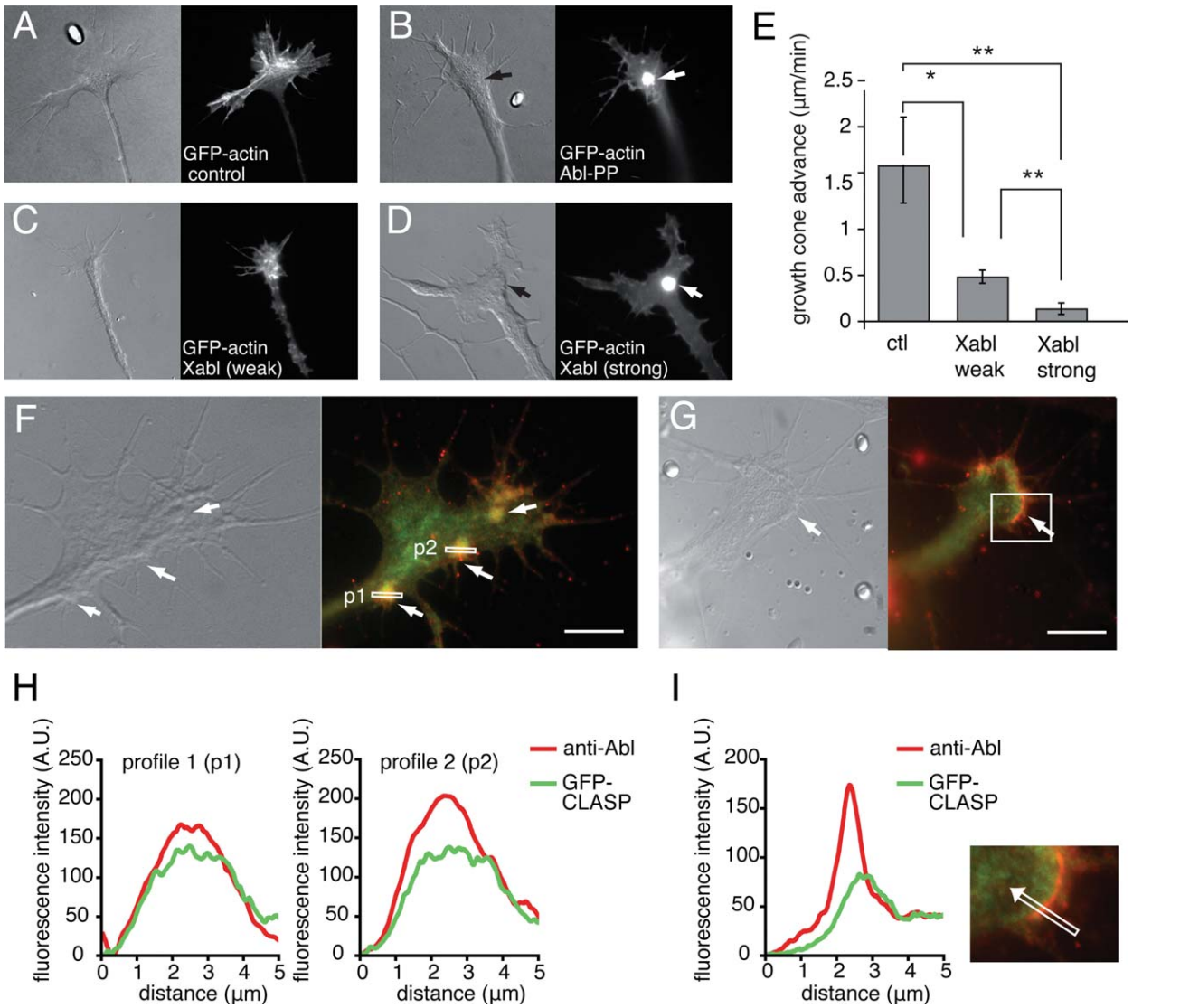

Fig. 8. Actin accumulates in Abl-induced adhesion plaques. A–D: Differential interference contrast (left side) and wide field fluorescence of GFP-actin of live growth cones which express GFP-actin only (A), GFP-actin co-expressed with constitutive active Abl (Abl-PP; **B**) or GFP-actin with Xenopus Abl (Xabl; **C** and D). The presence of Abl-induced adhesive plaques is indicated in bright field images (black arrows) and accumulation of GFP-actin (B, D) with white arrows. **E:** Quantification of growth cone advance in ctl, and Xabl growth cones which show adhesive plaques (as in D; Xabl strong), or weak actin accumulation (as in C; Xabl weak). Error bars represent standard error of the mean ($^{*}P < 0.025$, $^{**}P < 0.01$.) **F–G:** Immunolocalization of Abl (red) in growth cones expressing GFP-CLASP2γ (green) and Abl-PP with corresponding bright field images. Abl induced structures (white arrows) appear as round adhesive plaques (F) or as half circular fronts of Abl and CLASP2 accumulation (G, insert in I). **H,I:** Fluorescence intensity distribution of Abl and CLASP2 evaluated by intensity profiles (10 pixel integration). H: Intensity profiles shown in F as p1, p2. I: Profile across the ridge of the circular structure in G (region and direction of profile shown as arrow in insert). Scale bars are 10 µm.

of the growth cone along the *z*-direction revealed CLASP to be adjacent to the growth cone-substrate interface (see Supporting Information Fig. S5D, red arrow), consistent with sites of substrate adhesion.

Given the Abl-dependent enhancement of CLASP2 binding to actin we found in vitro, we examined actin distribution in growth cones expressing activated Abl by co-expressing GFP-actin (Fig. 8B) and compared it to wild type growth cones (Fig. 8A and Supporting Information Movie S4). We found a high degree of GFP-actin accumulation in the adhesive plaques induced by Abl-PP (Fig. 8B and Supporting Information Movie S5). To determine whether this reorganization of actin and the formation of adhesive plaques required constitutive Abl activity (Abl-PP), or was peculiar to expression of a mammalian Abl transgene, we also expressed wild type *Xenopus* Abl (Xabl) in the same spinal cord neurons. Unlike Abl-PP, Xabl displayed a more graded phenotype, where we found some growth cones with less distinct actin accumulation (Fig. 8C) in addition to many growth cones with dramatic actin accumulation in adhesive plaques indistinguishable from those observed with Abl-PP expression (Fig. 8D). There

was a strong correlation between the degree of actin accumulation with growth cone advance rates (Fig. 8E), suggesting that the rate of growth cone motility is proportional to the amount of Abl kinase activity. In growth cones where GFP-actin was recruited to the Abl-induced adhesive structure, growth cones showed very little forward movement (see Supporting Information Movie S5). Xabl expressing growth cones with less prominent actin accumulation moved faster than ones containing plaques, but still slower than control growth cones (Fig. 8E).

By immunolocalization of Abl in fixed growth cones, we also confirmed that Abl-PP colocalized together with GFP-CLASP2 in the adhesive plaques (Fig. 8F; intensity profiles in Fig. 8H). Abl-PP sometimes also formed ring-like structures in the growth cone (Fig. 8G), in which case CLASP was enriched in the same region (insert and profile in Fig. 8I). In summary, these structures induced by excessive Abl-activity, seemed to form a hub for Abl, CLASP, and actin accumulation and sequester CLASP away from MT plus ends.

Discussion

Genetic analysis of neural development in the *Drosophila* embryo showed previously that CLASP and other CLASP-interacting genes are important for the function of the Abl kinase signaling pathway [Lee et al., 2004; Lowery et al., 2010]; however, the mechanism and conservation of the functional link between Abl and CLASP was unknown. In the present study, we explore these questions. Our data indicate that Abl associates with and phosphorylates CLASP2 isoforms in vertebrate cells, and that this is influenced by activation of Abl by upstream factors. In vitro, we find that CLASP2 is a direct substrate of Abl with kinetics comparable to well-validated Abl substrates, and we identify sites of Abl phosphorylation embedded in a region containing both actin and MT + TIP binding domains of CLASP2. Using purified Abl and CLASP, we find that phosphorylation of CLASP2α modulates its binding to stabilized MTs and to F-actin. Finally, we observe that elevation of Abl activity in spinal cord growth cones induces a dramatic re-localization of CLASP2 away from MT plus ends in favor of cortical structures that become enriched in F-actin.

Genetic analysis of signaling pathways downstream of conserved receptors such as those in the Roundabout (Robo) and Leukocyte Antigen-Related (LAR) families can be a powerful tool to identify novel factors and determine their role in shaping cellular behavior in the context of the intact organism [Thompson and Van Vactor, 2006]. Indeed, our analysis of CLASP function in *Drosophila* central and peripheral axon pathway formation offered the first indication that the Abl kinase requires a MT-associated protein to mediate accurate guidance [Lee et al., 2004]. These data were consistent with observations of Abl-family localization and function in non-neuronal cells [Miller et al., 2009]. However, genetic assays rarely provide enough information alone to conclude a direct biochemical relationship exists. Thus, our finding that CLASP is bound to and phosphorylated by Abl in response to extracellular factors on a timescale of minutes is of particular importance for models placing CLASP directly downstream of the kinase. Moreover, our observation that the association of CLASP2 with cytoskeletal polymers in vitro can be regulated by Abl kinase activity reinforces the model that coordinated changes in MT and F-actin organization and dynamics are part of the downstream output of pathways (e.g., Robo, LAR, and others) that require Abl activity.

In biochemical assays and in *Xenopus* growth cones we find that Abl kinase activity enhances the association or co-localization of CLASP2 and F-actin, consistent with previous reports of CLASP binding to actin [Tsvetkov et al., 2007]. This is intriguing in light of recent observation that knock down of endogenous *Xenopus* CLASP disrupts actin distribution in the same class of neuronal growth cones [Marx et al., 2013]. In vivo genetic analysis in *Drosophila* has suggested that Abl and CLASP are part of a coordinated control of actin and MT effectors [Lee et al., 2004; Lowery et al., 2010]. Indeed, analysis of vertebrate cell movement has shown Abl-family kinases to coordinate the two polymer systems [Miller et al., 2004]. However, our MT-binding data and growth cone imaging indicate that while Abl may enhance CLASP2 binding to the MT lattice, it appears to antagonize the plus end tracking of CLASP2. Previous studies have shown that CLASP2 is subject to a kinase-dependent shift from MT lattice to MT plus end binding that appears to be important in developing and regenerating neurons [Wittmann and Waterman-Storer, 2005; Kumar et al., 2009; Hur et al., 2011]. Interestingly, the two conserved Abl phosphorylation sites that we mapped lie within the known MT plus end binding domain of CLASP2 [Mimori-Kiyosue et al., 2005; Wittmann and Waterman-Storer, 2005]. Future experiments will be required to determine whether these sites mediate the observed Abl-dependent changes in CLASP2 behavior as a prelude to dissecting the underlying mechanism.

In addition to identifying a direct mechanistic relationship between Abl and CLASP2, our results suggest that the functional link between Abl and CLASP is conserved across species. Our current observation that Abl and CLASP form a protein complex in vertebrate cells matches proteomic data from *Drosophila* cells [Lowery et al., 2010], suggesting that physical interactions are also conserved across phyla. While the precise phosphorylation sites observed in vertebrate CLASPs are not conserved in *Drosophila* Chb/Orbit/MAST, comparison of many signaling pathways between fly and mammals reveal that general mechanistic themes are frequently conserved. For example, despite poor conservation of specific Ena phosphoacceptor residues mapped in *Drosophila* cells [Gertler et al., 1995; Comer et al., 1998],

the functional linkage between Abl and the Enabled (Ena) family of proteins is conserved across species [Krause et al., 2004; Michael et al., 2010].

Materials and Methods

Antibodies and Reagents

The anti-phosphotyrosine (4G10) and anti-c-Abl (OPT20) antibodies were purchased from EMD Millipore (Billerica, MA) and used at 1:1000 and 1:250 dilutions, respectively, for Western blots. Anti-GFP (ab290, used at a 1:500 dilution), anti-tubulin (ab80779, used at a 1:5000 dilution), anti-beta actin (ab8224, used at a 1:5000 dilution), and anti-myc (ab9106, used at a 1:500 dilution) were purchased from Abcam (Cambridge, MA). The GFP-CLASP2α cDNA construct and anti-CLASP2 antibodies were generous gifts from Dr. Anna Akhmanova (Utrecht University, The Netherlands) and used at a 1:250 dilution for Western blots. Recombinant PDGF-BB (Abcam) was used at 100 ng/ml, protein tyrosine phosphatase 1b (PTP1B; Millipore) was used at 1 μg/μl and STI-571 (Novartis, Cambridge, MA) was used at 1 μM. A PDGF receptor inhibitor AG1296 was purchased from EMD Millipore and used at 1 μM final concentration.

Recombinant Protein Purification

Plasmid cDNAs of CLASP2α and CLASP2γ in pEGFP-C1 were obtained from Dr. Akhmanova [Akhmanova et al., 2001]. An NH2-terminal truncation of CLASP2γ was constructed using the internal restriction sites SacI (GFP-CLASPΔN-SacI). For generation of recombinant CLASP2γ protein, CLASP2γ cDNA was subcloned into pFastBac1 vector (Invitrogen, Grand Island, NY). 6xHis-CLASP2γ recombinant protein was produced in Hi-5 cells using the Bac-to-Bac expression system and purified with Ni-NTA agarose (Qiagen, Valencia, CA) according to procedures described by Tanis et al. [2003], followed by BioLogicDuo-flow gel filtration chromatography (Bio-Rad, Hercules, CA). The elution fractions were run on sodium dodecyl sulfate (SDS) poly acrylamide gels and stained with Coomassie blue. CLASP2α was amplified by PCR and subcloned into the pcDNA3.1-myc-His expression vector (Invitrogen) using Kpn and SacII restriction sites. The CLASP2α-myc-His construct was expressed in HEK293T cells for 24 h. Cells were solubilized and CLASP2α-myc-His was purified with a same procedure described for CLASP2γ.

In Vitro Kinase Assay

For the in vitro kinase assays (Fig. 3), a reaction mixture containing 25 mM HEPES (pH 7.25), 5% glycerol, 100 mM NaCl, 10 mM $MgCl_2$, 0.02 mg/ml BSA, 1 mM sodium orthovanadate, and 10 nM purified Abl (purified as described above; Tanis et al. [2003]) was incubated for 4 min at 37°C. To perform a time course to look at phosphorylation levels (Fig. 3B), a fixed concentration of CLASP2γ (25 nM) and 100 μM ATP was added and incubated at 37°C for varying amounts of time (0, 10, 20, 30, and 40 min) followed by SDS-PAGE and Western blot analysis using the anti-phosphotyrosine antibody 4G10. The reaction was stopped at 30 s by adding sample buffer and boiled for 5 min and followed by sodium dodecyl sulfate polyacrylamide gel electrophoresis (SDS-PAGE). The gels were dried, exposed for autoradiography, and the images were captured by a PhosphoImaging system (BioRad).

To investigate the cooperativity of Abl-dependent CLASP phosphorylation, variable amounts of CLASP2γ, 5 μM ATP and 0.5 μCi of γ-32P ATP were added into a 50 μl reaction (Figs. 3C and 3D). Data were fit to the Hill equation $(V_o = V_{max} \times [S]^h / (K_m^h + [S]^h)$ with K_m representing the concentration of CLASP at half-height. As the concentration of our proteins did not permit us to reach saturation, we constrained the curves (by setting V_{max} to 100) to give a lower bound for H and K_m, to compare CLASP with other substrates. The values we report are based on this lower bound. Quantitative results were obtained in six independent experiments performed on two different days with consistent results.

Cell Culture and DNA Transfection

HEK293T and COS7 cells were cultured in DMEM medium containing 10% fetal bovine serum (FBS) and 1% Penicillin/Streptomycin. Plasmid DNAs were transfected with Lipofectamin2000 transfection reagent (Invitrogen) according to manufacture's instructions. In a serum activation assay, 24 h post-transfection with GFP-CLASP2α, HEK 293T cells were transferred into serum-free medium. After 4 h, serum-free medium was replaced with serum- or PDGF-BB- (100 ng/ml) containing medium cells and cells were harvested after 2, 5, 10, or 30 min.

Immunoprecipitation

Cells were harvested and solubilized in 50 mM Tris-HCL containing 100 mM NaCl, 1% sodium deoxycholate, 0.5% Triton X-100, 1 mM $CaCl_2$, and complete protease inhibitor (Roche, Indianapolis, IN) and centrifuged for 37,000 × *g* for 30 min. About 60–100 μl of supernatant was precleared with 20 μl of protein G-agarose (Invitrogen) for 1 h. After preclearing, antibody to GFP or normal sera are added to the supernatants and incubated overnight at 4°C with constant shaking. About 40μl of protein G-agarose beads were then added and incubated for at least 1 h. The beads were pelleted by centrifugation at 4000 × *g* for 1 min and washed 3 × 10 min with solubilization buffer. The washed beads were boiled in 1× Laemmli sample buffer for 5 min and subjected to SDS-PAGE and Western blot analysis. Following SDS-PAGE, proteins were transferred to PVDF membrane, blocked for 1 h (Tris-buffered

saline/0.05% Tween 20 (TBST)/5% nonfat dry milk) and incubated overnight at 4°C in primary antibody solution Membranes were washed and incubated in the appropriate secondary antibody (HRP-conjugated secondary antibodies, 1:10,000, Jackson Immunoresearch, West Grove, PA) for 1 h at room temperature. Horseradish peroxidase was detected with enhanced chemiluminescence (GE Healthcare Life Sciences, Piscataway, NJ) and captured on autoradiographic film. For phosphorylation site identification, the gel of immunoprecipitated GFP-CLASP2α was stained with Coomassie-blue and the band of GFP-CLASP2α excised and sent for phospho-peptide mapping in Taplin Mass Spectrometry facility (Department of Cell Biology, Harvard Medical School, Boston, MA; see Supporting Information Fig. S2).

Polymerase Chain Reaction

To validate the presence of the phosphorylation site-containing fragment (amino acid 784–805) in mouse CLASP2β, primers were designed flanking amino acids 735–1030 (IDT DNA, Coralville, IA; Forward primer: TGTTGCTGTGGGAAATGCCAAGAC, Reverse primer: GCAGCTGTGTCAGCAGAACAAACA). To evaluate the expression of both long and short isoforms of CLASP2β, total RNA was harvested from mouse N2 cells and embryonic day 14 mouse tissues (brain, spinal cord, dorsal root ganglion, heart, liver, lung, and spleen) using Trizol reagent (Invitrogen). RNA was then reverse transcribed into cDNA (iScript, Bio-Rad Laboratories, Hercules, CA) and polymerase chain reaction (PCR) was performed using illustra PuReTaq Ready-To-Go PCR Beads (GE Healthcare Life Sciences). Ethidium bromide agarose gel electrophoresis was performed to evaluate PCR products. Bands corresponding to both long and short CLASP2β isoforms were gel purified (QIAquick Gel Extraction Kit, Qiagen) and sequenced (Dana Farber/Harvard Cancer Center DNA Sequencing Core, Boston, MA). Predicted amino acid sequences were determined using the ExPASy tool (Swiss Institute of Bioinformatics, web.expasy.org/translate).

Microtubule and Microfilament Co-sedimentation Assays

Tubulin monomers (5 mg/ml) were polymerized and stabilized with taxol as recommended (Cytoskeleton, Inc., Denver, CO). Twenty microliters of stabilized MTs (approximately 5.0×10^{11} MT/ml or 5 μM tubulin dimers) were incubated with 10 nM purified Abl and 50 nM purified CLASP2α-myc-His in a buffer containing 25 mM HEPES (pH 7.25), 100 mM NaCl, 10 mM $MgCl_2$, 1mM sodium orthovanadate, and 5 μM ATP at 37°C for 30 min. The reaction was transferred to 30% glycerol and centrifuged at 4°C for 30 min at 100,000 × *g*. The pellet and aliquots of supernatant were analyzed using SDS-PAGE and Western blot with antibodies to tubulin and myc. CLASP2α-myc-His was also incubated with the same buffer in the absence of stabilized MTs. The mixture was subjected to the same centrifugation conditions and the pellet and supernatant were analyzed as controls. Experiments were repeated a minimum of three times and relative intensities of bands representing proteins of interest were quantified using NIH Image J software [Rasband, 1997−2009]. The data were analyzed by Students *t*-test and reported as the mean ± standard deviation. Statistical significance was assumed when $P < 0.05$.

For the F-actin pelleting assay, actin monomers (Cytoskeleton, Inc.) were polymerized in 50 mM KCl, 1 mM ATP, and 2 mM $MgCl_2$ at room temperature for 1 h. Purified F-actin (21 μM) was incubated with CLASP2α in the presence or absence of Abl, STI-571 or protein tyrosine phosphatase (PTP1B) in the same buffer as the described above at 37°C for 30 min. The reaction was transferred to 30% glycerol and centrifuged at 4°C for 30 min at 100,000 × *g*. Equal amounts of pellet and samples of reaction prior to centrifugation were analyzed using SDS-PAGE and Western blot with anti-beta actin and anti-myc antibodies.

For the G-actin pelleting assay, tubulin monomers were polymerized, taxol-fixed and incubated with CLASP2α-myc-His and monomeric (G) actin (Cytoskeleton, Inc.; 21 μM) in the presence or absence of Abl, STI-571, or PTP1B in the same buffer as described above at 37°C for 30 min. The reaction was transferred to 30% glycerol and centrifuged at 4°C for 30 min at 100,000 × *g*. Equal amounts of pellet and samples of reaction before centrifugation were analyzed using SDS-PAGE and Western blot with anti-beta actin, anti-tubulin, and anti-myc antibodies.

Xenopus Neuronal Culture

Capped RNA for injection was transcribed from linearized plasmids with the mMessage mMachine Kit (Ambion). The RNA was then purified with Qiagen RNeasy Mini Kit and a subsequent ethanol precipitation step. Capped RNA of GFP-CLASP2γ was injected at 0.5–1 ng, GFP-actin- at 0.25 ng, Xabl at 0.8 ng, and Abl-PP at 50 pg per blastomere. Even at 50 pg of Abl-PP up to 30% of injected embryos showed incomplete gastrulation and spina bifida phenotypes. Injections of mRNA and neuronal culture on laminin-coated glass coverslips were performed as described [Lee et al., 2004]. Growth cones were fixed in 4% paraformaldehyde (PFA) in Krebs buffer supplemented with 0.4M sucrose for 20 min. After the membranes were opened with 0.25% Triton-X in PBS, growth cones were incubated in blocking solution (5% heat inactivated normal goat serum in PBS) to prevent nonspecific antibody binding. Growth cones were incubated in primary antibody solution (anti-Abl, 1:100 diluted in blocking buffer) overnight at 4°C. Following three washes in PBS, samples were incubated in secondary antibody (goat anti-mouse Alexa Fluor 568, 1:400 diluted in blocking buffer) for 1 h at room

temperature. Note that with PFA fixation, CLASP plus end localization is only poorly conserved. For this reason, the CLASP localization study in Fig. 7 was performed on live growth cones.

Microscopy and Image Analysis

Dynamic imaging of growth cones was performed with a ×100 NA 1.4 objective on a Nikon TE300 equipped with automated excitation and emission filter wheels for multichannel time-lapse (Ludl Inc.). Image acquisition on an OrcaER camera (Hamamatsu) was controlled by Openlab3 (Improvision). The illumination of a 100 W Mercury lamp was attenuated to 5–20% with neutral density filters and shuttered to 0.1–0.8 ms exposure times to prevent photodamage in growth cones. For the three-dimensional (3D) analysis in Fig. 7, live growth cones were imaged with an Ultraview ERS spinning disk confocal (Perkin Elmer LAS) on a Nikon TE2000-E inverted microscope equipped with a Plan-Apochromat VC ×100 lens (NA 1.4). Channels were recorded sequentially onto an EM-CCD camera using 488 nm excitation, 527/55 nm emission and 568 nm excitation, 615/70 nm emission for EGFP, and Alexa 568 labels, respectively. Optical slices were acquired at 0.15-µm *z*-spacing generating a stack of approximately 30–40 slices per cell. These stacks were deconvolved based on a theoretical point spread function (PSF) using Huygens Essential software version 3.0 (Scientific Volume Imaging BV). 3-D Projections of deconvolved data were generated as maximum intensity projections as indicated. Volumes of high CLASP2 localization were visualized by 3D iso-data thresholding (iso-data). Orthogonal views in *xz* and *xy* as well as the intensity analysis were performed with Image J [Rasband, 1997−2009].

Acknowledgments

Authors are grateful to Novartis for the gift of compound STI-571 used in the initial experiments. They also thank Drs. Anna Akhmanova, Niels Galjart, and Irina Kaverina for CLASP reagents and Dr. Daniela Barila for the Abl-PP construct, April Duckworth for technical assistance, and the Niehrs Lab at the DKFZ for *Xenopus* embryos and injection facilities. Authors thank the Nikon Imaging Centers at Harvard Medical School and at the University of Heidelberg for use of microscopy instruments and support. YZ, UE, and DVV were funded by NIH grant R01-NS35909; JBL was funded by NIH grant T32-CA009361-30.

References

Akhmanova A, Hoogenraad CC, Drabek K, Stepanova T, Dortland B, Verkerk T, Vermeulen W, Burgering BM, De Zeeuw CI, Grosveld F, et al. 2001. Clasps are CLIP-115 and -170 associating proteins involved in the regional regulation of microtubule dynamics in motile fibroblasts. Cell 104(6):923–935.

Barila D, Superti-Furga G. 1998. An intramolecular SH3-domain interaction regulates c-Abl activity. Nat Genet 18(3):280–282.

Bashaw GJ, Kidd T, Murray D, Pawson T, Goodman CS. 2000. Repulsive axon guidance: Abelson and Enabled play opposing roles downstream of the roundabout receptor. Cell 101(7):703–715.

Baum B, Perrimon N. 2001. Spatial control of the actin cytoskeleton in Drosophila epithelial cells. Nat Cell Biol 3(10):883–890.

Bear JE, Loureiro JJ, Libova I, Fassler R, Wehland J, Gertler FB. 2000. Negative regulation of fibroblast motility by Ena/VASP proteins. Cell 101(7):717–728.

Boyle SN, Michaud GA, Schweitzer B, Predki PF, Koleske AJ. 2007. A critical role for cortactin phosphorylation by Abl-family kinases in PDGF-induced dorsal-wave formation. Curr Biol 17(5):445–451.

Colicelli J. 2010. ABL tyrosine kinases: Evolution of function, regulation, and specificity. Sci Signal 3(139):re6.

Comer AR, Ahern-Djamali SM, Juang JL, Jackson PD, Hoffmann FM. 1998. Phosphorylation of Enabled by the Drosophila Abelson tyrosine kinase regulates the in vivo function and protein-protein interactions of Enabled. Mol Cell Biol 18(1):152–160.

Drabek K, van Ham M, Stepanova T, Draegestein K, van Horssen R, Sayas CL, Akhmanova A, Ten Hagen T, Smits R, Fodde R, et al. 2006. Role of CLASP2 in microtubule stabilization and the regulation of persistent motility. Curr Biol 16(22):2259–2264.

Druker BJ, Tamura S, Buchdunger E, Ohno S, Segal GM, Fanning S, Zimmermann J, Lydon NB. 1996. Effects of a selective inhibitor of the Abl tyrosine kinase on the growth of Bcr-Abl positive cells. Nat Med 2(5):561–566.

Efimov A, Kharitonov A, Efimova N, Loncarek J, Miller PM, Andreyeva N, Gleeson P, Galjart N, Maia AR, McLeod IX, et al. 2007. Asymmetric CLASP-dependent nucleation of noncentrosomal microtubules at the trans-Golgi network. Dev Cell 12(6):917–930.

Elkins T, Zinn K, McAllister L, Hoffmann FM, Goodman CS. 1990. Genetic analysis of a Drosophila neural cell adhesion molecule: interaction of fasciclin I and Abelson tyrosine kinase mutations. Cell 60(4):565–755.

Gertler FB, Bennett RL, Clark MJ, Hoffmann FM. 1989. Drosophila abl tyrosine kinase in embryonic CNS axons: A role in axonogenesis is revealed through dosage-sensitive interactions with disabled. Cell 58(1):103–113.

Gertler FB, Comer AR, Juang JL, Ahern SM, Clark MJ, Liebl EC, Hoffmann FM. 1995. enabled, a dosage-sensitive suppressor of mutations in the Drosophila Abl tyrosine kinase, encodes an Abl substrate with SH3 domain-binding properties. Genes Dev 9(5): 521–533.

Gundersen GG. 2002. Evolutionary conservation of microtubule-capture mechanisms. Nat Rev Mol Cell Biol 3(4):296–304.

Harbott LK, Nobes CD. 2005. A key role for Abl family kinases in EphA receptor-mediated growth cone collapse. Mol Cell Neurosci 30(1):1–11.

Heng YW, Koh CG. 2010. Actin cytoskeleton dynamics and the cell division cycle. Int J Biochem Cell Biol 42(10):1622–1633.

Hernandez SE, Krishnaswami M, Miller AL, Koleske AJ. 2004. How do Abl family kinases regulate cell shape and movement? Trends Cell Biol 14(1):36–44.

Hur EM, Saijilafu, Lee BD, Kim SJ, Xu WL, Zhou FQ. 2011. GSK3 controls axon growth via CLASP-mediated regulation of growth cone microtubules. Genes Dev 25(18):1968–1981.

Jiang K, Akhmanova A. 2011. Microtubule tip-interacting proteins: A view from both ends. Curr Opin Cell Biol 23(1):94–101.

Kodama A, Lechler T, Fuchs E. 2004. Coordinating cytoskeletal tracks to polarize cellular movements. J Cell Biol 167(2):203–207.

Komarova YA, Akhmanova AS, Kojima S, Galjart N, Borisy GG. 2002. Cytoplasmic linker proteins promote microtubule rescue in vivo. J Cell Biol 159(4):589–599.

Krause M, Leslie JD, Stewart M, Lafuente EM, Valderrama F, Jagannathan R, Strasser GA, Rubinson DA, Liu H, Way M, et al. 2004. Lamellipodin, an Ena/VASP ligand, is implicated in the regulation of lamellipodial dynamics. Dev Cell 7(4):571–583.

Kumar P, Lyle KS, Gierke S, Matov A, Danuser G, Wittmann T. 2009. GSK3beta phosphorylation modulates CLASP-microtubule association and lamella microtubule attachment. J Cell Biol 184(6): 895–908.

Lee H, Engel U, Rusch J, Scherrer S, Sheard K, Van Vactor D. 2004. The microtubule plus end tracking protein Orbit/MAST/CLASP acts downstream of the tyrosine kinase Abl in mediating axon guidance. Neuron 42(6):913–926.

Lowery LA, Lee H, Lu C, Murphy R, Obar RA, Zhai B, Schedl M, Van Vactor D, Zhan Y. 2010. Parallel genetic and proteomic screens identify Msps as a CLASP-Abl pathway interactor in Drosophila. Genetics 185(4):1311–1325.

Marx A, Godinez WJ, Tsimashchuk V, Bankhead P, Rohr K, Engel U. 2013. Xenopus cytoplasmic linker-associated protein 1 (XCLASP1) promotes axon elongation and advance of pioneer microtubules. Mol Biol Cell 24(10):1544–1558.

Michael M, Vehlow A, Navarro C, Krause M. 2010. c-Abl, Lamellipodin, and Ena/VASP proteins cooperate in dorsal ruffling of fibroblasts and axonal morphogenesis. Curr Biol 20(9):783–791.

Miller AL, Wang Y, Mooseker MS, Koleske AJ. 2004. The Abl-related gene (Arg) requires its F-actin-microtubule cross-linking activity to regulate lamellipodial dynamics during fibroblast adhesion. J Cell Biol 165(3):407–419.

Miller PM, Folkmann AW, Maia AR, Efimova N, Efimov A, Kaverina I. 2009. Golgi-derived CLASP-dependent microtubules control Golgi organization and polarized trafficking in motile cells. Nat Cell Biol 11(9):1069–1080.

Mimori-Kiyosue Y, Grigoriev I, Lansbergen G, Sasaki H, Matsui C, Severin F, Galjart N, Grosveld F, Vorobjev I, Tsukita S, et al. 2005. CLASP1 and CLASP2 bind to EB1 and regulate microtubule plus-end dynamics at the cell cortex. J Cell Biol 168(1):141–153.

Moresco EM, Scheetz AJ, Bornmann WG, Koleske AJ, Fitzsimonds RM. 2003. Abl family nonreceptor tyrosine kinases modulate short-term synaptic plasticity. J Neurophysiol 89(3):1678–1687.

Moresco EM, Donaldson S, Williamson A, Koleske AJ. 2005. Integrin-mediated dendrite branch maintenance requires Abelson (Abl) family kinases. J Neurosci 25(26):6105–6118.

Patel K, Nogales E, Heald R. 2012. Multiple domains of human CLASP contribute to microtubule dynamics and organization in vitro and in Xenopus egg extracts. Cytoskeleton (Hoboken) 69(3): 155–165.

Plattner R, Kadlec L, DeMali KA, Kazlauskas A, Pendergast AM. 1999. c-Abl is activated by growth factors and Src family kinases and has a role in the cellular response to PDGF. Genes Dev 13(18):2400–2411.

Rasband W. 1997−2009. ImageJ. Bethesda, MD: U.S. National Institutes of Health. http://rsb.info.nih.gov/ij/.

Rodriguez OC, Schaefer AW, Mandato CA, Forscher P, Bement WM, Waterman-Storer CM. 2003. Conserved microtubule-actin interactions in cell movement and morphogenesis. Nat Cell Biol 5(7):599–609.

Shimizu A, Mammoto A, Italiano JE Jr, Pravda E, Dudley AC, Ingber DE, Klagsbrun M. 2008. ABL2/ARG tyrosine kinase mediates SEMA3F-induced RhoA inactivation and cytoskeleton collapse in human glioma cells. J Biol Chem 283(40):27230–27238.

Tanis KQ, Veach D, Duewel HS, Bornmann WG, Koleske AJ. 2003. Two distinct phosphorylation pathways have additive effects on Abl family kinase activation. Mol Cell Biol 23(11):3884–3896.

Thompson C, Van Vactor D. 2006. Abelson family protein tyrosine kinases and the formation of neuronal connectivity. In: Koleske AJ, editor. Abl Family Kinases in Development and Disease. Landes Bioscience, Georgetown, TX and Springer Science + Business Media, New York, NY. pp 105–122.

Toyofuku T, Zhang H, Kumanogoh A, Takegahara N, Yabuki M, Harada K, Hori M, Kikutani H. 2004. Guidance of myocardial patterning in cardiac development by Sema6D reverse signalling. Nat Cell Biol 6(12):1204–1211.

Tsvetkov AS, Samsonov A, Akhmanova A, Galjart N, Popov SV. 2007. Microtubule-binding proteins CLASP1 and CLASP2 interact with actin filaments. Cell Motil Cytoskeleton 64(7):519–530.

Wills Z, Bateman J, Korey CA, Comer A, Van Vactor D. 1999a. The tyrosine kinase Abl and its substrate enabled collaborate with the receptor phosphatase Dlar to control motor axon guidance. Neuron 22(2):301–312.

Wills Z, Marr L, Zinn K, Goodman CS, Van Vactor D. 1999b. Profilin and the Abl tyrosine kinase are required for motor axon outgrowth in the Drosophila embryo. Neuron 22(2):291–299.

Wittmann T, Waterman-Storer CM. 2005. Spatial regulation of CLASP affinity for microtubules by Rac1 and GSK3beta in migrating epithelial cells. J Cell Biol 169(6):929–939.

Yu HH, Zisch AH, Dodelet VC, Pasquale EB. 2001. Multiple signaling interactions of Abl and Arg kinases with the EphB2 receptor. Oncogene 20(30):3995–4006.